Self-phase modulation and optical pulse compression influenced by stimulated Raman scattering in fibers

A. M. Weiner and J. P. Heritage

Bell Communications Research, 331 Newman Springs Road, Red Bank, New Jersey 07701-7020

R. H. Stolen

AT&T Bell Laboratories, Crawfords Corner Road, Holmdel, New Jersey 07733

Received May 4, 1987; accepted August 3, 1987

We have investigated experimentally the influence of stimulated Raman scattering, under conditions of pulse walk-off, on the propagation of mode-locked 1.06-μm pulses in single-mode, polarization-preserving fibers and on their subsequent pulse compression. Intense stimulated Raman scattering preferentially depletes (and steepens) the leading edge of 1.06-μm pump pulses and clamps the pump pulse energy. Subsequent self-phase modulation of the reshaped pump leads to nonsymmetric spectral broadening and to a nonlinear chirp. Nevertheless, high-quality compressed pulses may be obtained by using an asymmetric spectral window to select a subset of the broadened spectrum. The best compression is achieved when the downshifted spectral components, corresponding to the portion of the pump pulses most severely depleted by stimulated Raman scattering, are selected. Such pulse compression performed under conditions of strong Raman conversion is highly stabilized compared with conventional pulse compression.

1. INTRODUCTION

Two of the most important nonlinear processes that occur in single-mode optical fiber are self-phase modulation[1] (SPM) and stimulated Raman scattering[2] (SRS). SPM forms the basis for the fiber and grating pulse compressor,[3,4] which is now an established tool in ultrafast pulse technology. SRS is useful for frequency-conversion applications[5,6] but competes with SPM and limits the power of optical pulses in fibers.[7] Although a number of groups have investigated Raman scattering stimulated by ultrashort pulses in fibers,[8–14] there has been little study of the effect of SRS on pulse compression. Nevertheless, researchers have generally agreed that SRS must be avoided if high-quality pulse compression is to be achieved.[13,14]

In this paper, we carefully examine picosecond pulse depletion by SRS in single-mode fibers and the implications for subsequent compression of the SPM chirped pulses. We find that compression of pulses clamped by extreme SRS is highly stabilized compared with conventional pulse compression. Stimulated Raman scattering of short optical pulses is modified by group-velocity dispersion (GVD), which causes walk-off of the generated Stokes pulse from the incident pulse.[10,11] Under conditions of walk-off with normal disperson, intense SRS preferentially depletes the leading edge of the pump pulse, clamping the pump-pulse energy and steepening its rising edge. SPM of the reshaped pump pulses causes the nonsymmetric spectral broadening observed in several experiments[10,12–15] and a nonlinear chirp. Despite the nonlinear chirp, high-quality pulse compression may be achieved by using an asymmetric spectral window[16] to eliminate blue-shifted spectral components.

The fiber length we chose for these experiments is sufficiently short that broadening of the pump pulse due to GVD is not a factor. In these circumstances the sole effect of GVD is to introduce walk-off between Stokes and pump pulses. In a subsequent paper, we plan to describe the effect of SRS on SPM and pulse compression in longer fibers, for which pulse broadening due to GVD must be considered.[17] The current investigation of pulse compression, as influenced by SRS in shorter fibers, will serve as a foundation for examination of new phenomena that arise because of the combined influence of SRS and GVD in longer fibers.

2. EXPERIMENT

The experimental apparatus employs a double-pass fiber and grating pulse compressor[18] similar to that used in our previous investigation of spectral windowing[16] and pulse shaping[19,20] in a grating compressor. The setup is sketched in Fig. 1. 75-psec, 1.06-μm pulses from a cw-mode-locked Nd:YAG laser, at a repetition rate of 100 MHz, were coupled into a 145-m length of single-mode, polarization-preserving fiber. Fiber parameters are given in Appendix B of Ref. 21. We chose a length of fiber that would exceed the length for walk-off between Stokes and pump pulses but would be sufficiently short that the effect of GVD on the pump pulses itself could be neglected. The SPM spectrum of the pump pulse was monitored using a photodiode array to measure the spatially dispersed spectrum present after a single pass through the grating compressor. A 1-m monochromator was used for high-resolution spectral measurements. The temporal profile of the Stokes and pump pulses emerging from the fiber were measured with a high-speed InGaAs P–I–N photodiode[22] and a sampling oscilloscope, which together had a 10–90% rise time of 28 psec (calibrated using 3-psec compressed pulses). To observe the pump pulse or the Stokes pulse individually, a four-prism arrangement[23] was inserted before the photodiode to serve as a spectral filter.

0740-3224/88/020364-09$02.00

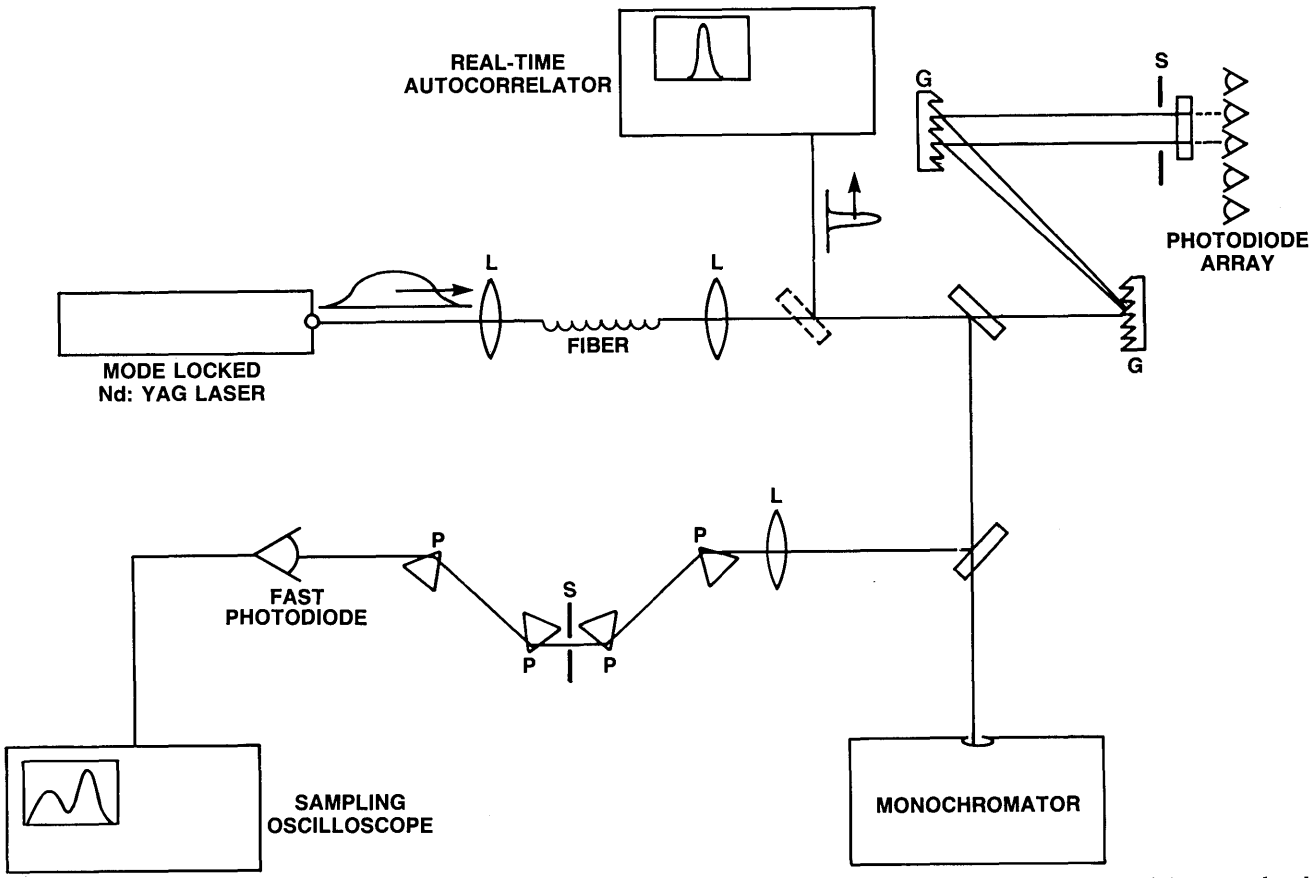

Fig. 1. Experimental apparatus used to investigate the influence of stimulated Raman scattering on self-phase modulation and pulse compression: G's, gratings; L's, lenses; P's, prisms; S's, slits.

Midway through the prism arrangement, the optical beam was brought into focus, and a knife edge was used to block either the pump or the Stokes light.

For the pulse-compression experiments, a spinning-block real-time autocorrelator was used as a continuous monitor of the compressed pulse width. More accurate pulse-width measurements were performed using a stepper-motor-driven delay line and signal averager. We used a modified compressor setup, described in Ref. 20, in order to have two distinct compressed pulses available, each of which could be spectrally windowed using its own independently adjustable window. Cross-correlation measurements between these individually windowed pulses were performed to clarify the effects of the spectral windowing.

We estimated the pump power at the input end of the fiber by measuring the total power emerging from the output of the fiber; the propagation loss in the 145-m fiber is only a few percent. In our experiments, the pump power was adjusted from 0 to 2 W average (270 W peak). The threshold for SRS was ~870 mW. At the highest power, the Raman conversion is 60%; at this point, a 5% overall conversion efficiency to second Stokes is observed.

3. EFFECT OF SRS ON THE PUMP PULSE

A. Pump-Pulse Reshaping

The reshaping of the pump pulse owing to SRS is mainly influenced by two processes: walk-off and pump depletion. Walk-off[10,11] is illustrated in Fig. 2, which shows the temporal separation of Stokes and pump pulses emerging from the fiber, for the case of high (46%) Raman conversion. The Raman pulse precedes the 1.06-μm pulse by 181 psec. Referenced to a pump pulse attenuated below the Raman threshold, the separation would be 162 psec. The additional 19-psec separation may be attributed to an apparent delay of the pump pulse owing to depletion of its leading edge. The

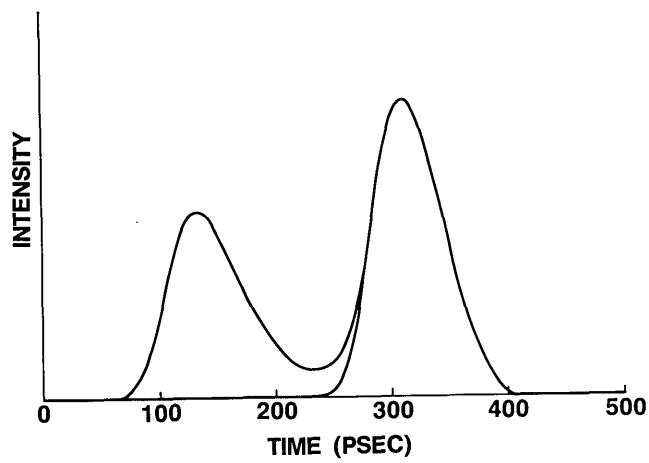

Fig. 2. High-speed photodiode measurement of 1.06-μm and Stokes-shifted 1.12-μm pulses emerging from 145-m fiber. The 1.12-μm pulse arrives 205 psec before the 1.06-μm pump pulse.

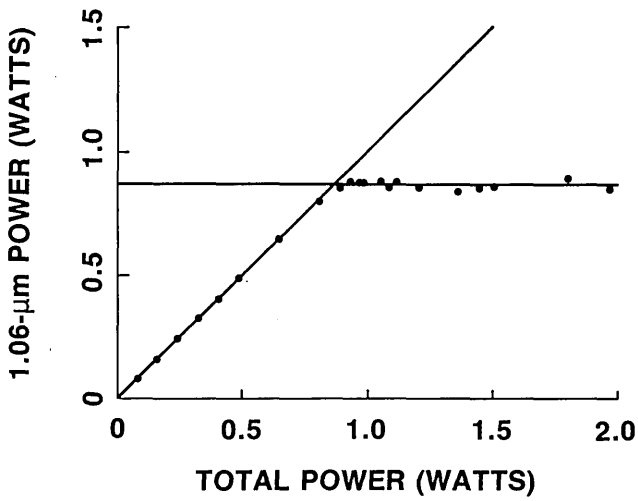

Fig. 3. Clamping of the 1.06-μm pump-pulse energy by stimulated Raman scattering. The 1.06-μm pulse energy emerging from the fiber is plotted versus the total energy (1.06-μm energy as well as Stokes-shifted energy) emerging from the fiber.

walk-off of 162 psec is consistent with the frequency shift of 440 cm^{-1}, the estimated dispersion of 1.5 psec/m, and the observation[8,10] that the Stokes pulse is generated one to two walk-off lengths into the fiber. For a 75-psec input pulse, the walk-off length (defined as the distance for the Stokes pulse and pump pulse to separate by one input pulse width) is 49 m.

Clamping of the pump energy is demonstrated in Fig. 3, which plots the 1.06-μm power exiting the fiber as a function of total energy. Above the Raman threshold, further increases in pump energy result only in increased Raman conversion. We see that stimulated Raman scattering is a remarkably good hard-limiter. However, pulse walk-off is required to obtain data such as shown in Fig. 3. For SRS without walk-off, the final pump energy not only levels off but eventually drops to zero as the input pump energy is increased further above threshold.[24,25]

This difference between SRS with and without walk-off may be understood from an estimate of the Raman gain. With no walk-off, the unsaturated Raman gain g is equal to

$$g = \gamma \frac{P_o L}{A_{\text{eff}}}, \tag{1}$$

where γ is the peak Raman gain coefficient, P_o is the peak pump power, A_{eff} is the effective area, and L is the fiber length. The gain depends on the peak intensity. With walk-off, however, the Raman pulse sees the entire pump pulse. In the limit where the Stokes walks completely through the pump, and without pump depletion, the gain g is given by

$$g = \frac{\gamma}{|\alpha|} \int \frac{P(t)}{A_{\text{eff}}} \, dt = \frac{\gamma U_p}{|\alpha| A_{\text{eff}}}, \tag{2}$$

where

$$\alpha = (1/v_g)|_{\text{Stokes}} - (1/v_g)|_{\text{pump}}$$

is the inverse walk-off velocity, and U_p is the pump-pulse energy. Thus, in the case of walk-off, the gain depends on the pump-pulse energy, not on the peak intensity. Above the Raman threshold, apparently, strong SRS depletes the pump energy just enough to maintain a constant gain. This effect clamps the pump energy and, as we shall see, can be helpful in stabilizing the pulse-compression process.

Together walk-off and strong Raman conversion cause reshaping of the pump pulse.[11-14] Because the Raman pulse reaches its highest intensity as it passes through the front of the pump pulse, the leading edge of the pump is depleted preferentially. This action results in an asymmetric pump pulse with a steepened leading edge. Figure 4(A) shows the pump intensity profile at the output end of the fiber for two power levels. The solid line corresponds to 800-mW average power, below the onset of SRS. The dashed line corresponds to 1.7-W total power, with 49% conversion to Raman. The dashed curve is shorter and more intense, with a sharpened leading edge. The deconvolved 10–90% rise time of the reshaped pulse is 30 psec, compared with a rise time of 52 psec in the absence of SRS. The effect of pump depletion is revealed graphically by Fig. 4(B), which shows the same two curves, but with the low-power curve scaled up by a factor of 2.1 so that its intensity matches that of the higher-power pulse before depletion. Figure 4(B) shows that strong SRS eliminates, nearly completely, the leading portion of the pump pulse and leaves the trailing edge of the pump unaltered.

Raman walk-off will occur in pulse-compression experiments under a wide range of conditions. Optimum compression is generally achieved when the spectrally broadened pulse in the fiber is temporally broadened by GVD. For compressed pulse lengths exceeding approximately 30 fsec, the Raman frequency shift in silica core fibers will exceed the pulse bandwidth. Therefore, for optimum compression to pulse widths above 30 fsec, Raman scattering, if it occurs, will occur under conditions of pulse walk-off.

B. Nonsymmetric Spectra

Because the pump pulse is reshaped, the onset of SRS is linked to a nonsymmetric spectral broadening of the pump.[11,14] This nonsymmetric spectral broadening is depicted in Fig. 5, which shows a sequence of power spectra for increasing pump powers. These spectra were measured us-

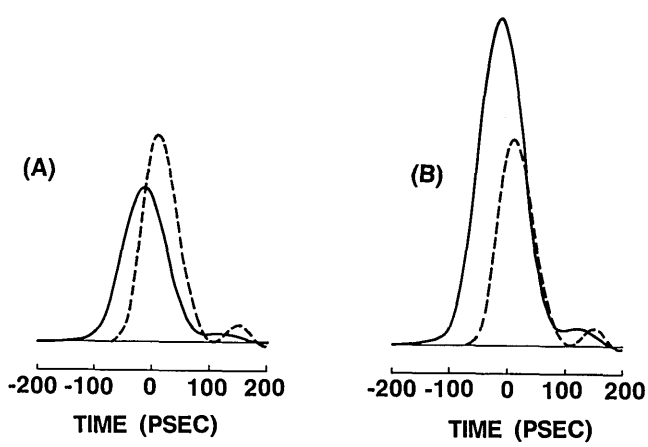

Fig. 4. Pump-pulse reshaping by stimulated Raman scattering. The solid line shows the pump-pulse shape below the Raman threshold; the dashed line shows the reshaped pump with intense SRS. (A) Both curves are plotted with the same vertical scale. (B) The solid unshaped pulse is scaled so that its energy matches that of the shaped pulse prior to depletion.

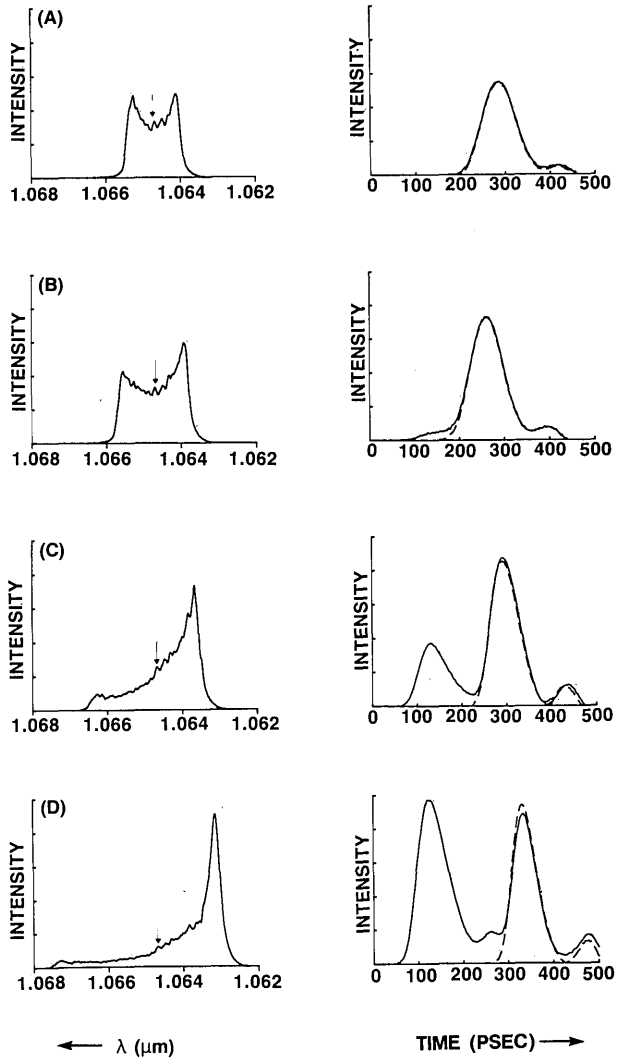

Fig. 5. Nonsymmetric spectral broadening due to stimulated Raman scattering. The traces on the left are power spectra measured using the photodiode array positioned after a single pass through the grating pair; the arrows indicate the position of the carrier frequency. The traces on the right are the corresponding pulse intensity profiles; solid lines indicate both 1.06-μm and Raman present and dashed lines indicate Raman blocked. The power increases from top to bottom: (A), 700-mW pump power, no Raman conversion; (B), 955-mW pump power, 11% conversion; (C), 1.27-W pump power, 35% conversion; and (D), 1.89-W pump power, 60% conversion.

ing the photodiode array situated midway through the pulse compressor apparatus. Also shown is the corresponding sequence of pulse intensity profiles, with and without the Raman pulse blocked. Below the Raman threshold [Fig. 5(A)], the self-phase modulation is symmetric. At threshold and slighty above [11% Raman conversion, Fig. 5(B)], the spectrum begins to droop toward the longer wavelengths. In Figs. 5(C) and 5(D), the Raman conversion is 35 and 60%, respectively, and the Raman pulse has separated from the pump. In these data, the droop toward longer wavelengths is substantial; in addition, the red-shifted spectral broadening now exceeds the blue-shifted broadening. In Fig. 5(D), the red-shifted broadening is 25.6 Å, and the blue-shifted broadening is 18.7 Å.

Two distinct mechanisms may be invoked to explain such nonsymmetric spectral broadening. The first mechanism arises due to simultaneous SRS and SPM. Since SRS preferentially depletes the leading edge of the pump pulse, red-shifted frequencies, which are created in the front edge of the pump, are also preferentially depleted. This process, which was also proposed by other authors,[14] explains the droop on the Stokes side of the spectrum but cannot account for the greater broadening on the Stokes side. The second mechanism, which can explain the more extensive Stokes broadening, considers SRS and SPM as a two-step process. In the first part of the fiber, SRS occurs, causing depletion and reshaping of the pump pulse. In the second part of the fiber, spectral broadening due to SPM of the reshaped pump pulse takes place. SRS is assumed not to occur in this second portion of the fiber because of the effect of walk-off and pump depletion. In this picture, the asymmetry of the reshaped pump pulse yields a nonsymmetric SPM spectrum. Because the instantaneous frequency is the time derivative of the nonlinear phase shift, the red-shifted spectral broadening produced by the fast rising edge of the pump pulse exceeds the blue-shifted broadening produced by the slower trailing edge. Furthermore, since the depleted leading portion of the pulse contains a minority of the pulse energy yet contributes a majority of the spectral broadening, the spectrum must droop toward longer wavelengths.

Although both mechanisms do affect the pump SPM spectrum, the relative importance of these two mechanisms depends on pump intensity. The spectra begin to droop at and slightly above the onset of SRS, before appreciable asymmetry in the broadening is observed. For these power levels, the first mechanism, involving simultaneous SPM and SRS, appears to be important. This mechanism would be consistent with a Raman pulse generated relatively late in the fiber, which does not cleanly separate from or greatly reshape the pump. The second mechanism, which involves sequential SRS and SPM, appears to dominate at higher power levels with strong Raman conversion. At intensities well above the threshold for SRS, Raman generation and pump-pulse reshaping occur early in the fiber, and the Raman pulse walks off cleanly from the pump. Under these conditions, large asymmetry is observed in the spectral broadening. Mechanism two, an initial reshaping of the pump by SRS followed by generation of a nonsymmetric SPM spectrum, may be primarily responsible for the nonsymmetric spectral broadening observed in pulse-compression experiments involving Nd:YAG lasers[10,12–14] as well as dye lasers.[15] We reiterate that the first mechanism, proposed by others to explain the droop toward longer wavelengths, cannot alone explain the observed asymmetric spectral broadening.

Further information is obtained when broadened spectra corresponding to strong Raman conversion are measured with high spectral resolution. A spectrum measured using the 1-m monochromator is plotted in Fig. 6(A) and exhibits a distinct discontinuity at the original carrier frequency. The 1-8-Å period oscillations are a Fabry–Perot artifact due to a neutral-density filter in the beam. The shape of the spectrum, including the discontinuity at the carrier frequency, brings to mind a pump pulse composed of two distinct halves, with differing pulse widths, pasted together. We have calculated a similar spectrum by allowing SPM to operate on an initially asymmetric pulse with the assumption of

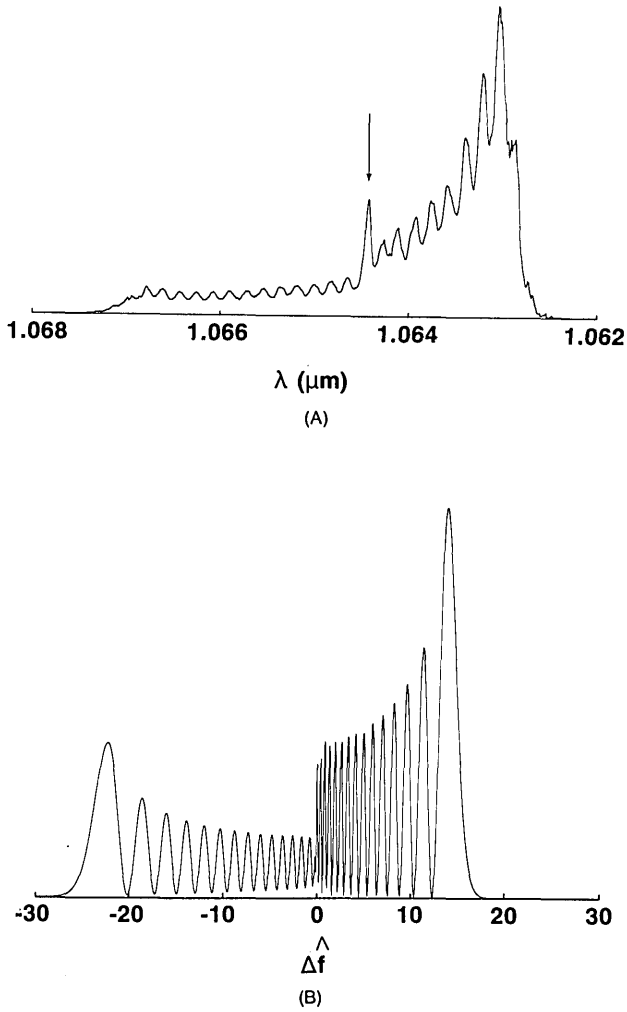

Fig. 6. (A) High-resolution power spectrum measurement using 1-m monochromator. The Raman conversion is >50%. Note the discontinuity at the carrier frequency (indicated by the arrow). The 1.8-Å period oscillations are a Fabry–Perot artifact due to a neutral-density filter. (B) Calculated self-phase modulation spectrum of an asymmetric secant hyperbolic pulse, defined by Eq. (3). The parameters are $b = 3$, $t_o = 34$ psec, and G = 90.

negligible GVD. For this calculation, we used an asymmetric secant hyperbolic pulse shape, given by

$$I(t) = \left[\frac{A}{\exp(-bt/t_o) + \exp(t/t_o)}\right]^2, \tag{3}$$

where $A = b^{1/(1+b)} + b^{-b/(1+b)}$ is a normalization coefficient. The constants b and t_o were set to $b = 3$ and $t_o = 34$ psec in order to match the measured pump-pulse shape at the fiber exit and to fit the asymmetry and width of the spectrum in Fig. 6(A). The spectrum was best fit using a SPM coefficient $G = 90$, defined by the relation $\phi(t) = GI(t)$, where $\phi(t)$ is the intensity-dependent phase.

The spectrum calculated using these parameters is plotted in Fig. 6(B). The agreement between calculated and measured spectra supports the contention that mechanism two is dominant for cases of strong Raman conversion. Similar asymmetric spectra, with discontinuities, were discussed as far back as 1970, in connection with SPM of picosecond pulses trapped in self-focused filaments.[26]

4. IMPLICATION FOR PULSE COMPRESSION

In Section 3 we described the effect of SRS on pump-pulse SPM: namely, that strong SRS preferentially depletes (hence steepens) the leading edge of the pump pulse and that SPM of the reshaped pulse leads to nonsymmetric spectral broadening. In this section we discuss the implications for pulse compression. Although it has been generally accepted that SRS must be avoided if effective pulse compression is to be achieved,[13,14] we show that high-quality compressed pulses may be obtained under conditions of intense SRS by use of an asymmetric spectral window. We also report the startling result that highly stabilized compression may be achieved by operating under conditions of strong SRS.

Effective pulse compression requires generation of a linear chirp that can be compensated by a grating pair. Asymmetry of the initial pulse on which SPM operates would be expected to detract from the linearity of the chirp. By using the same parameters used to calculate Fig. 6(B) and assuming zero GVD, we have calculated the instantaneous frequency profile developed by the pulse defined in Eq. (3). The result is plotted in Fig. 7(A), with dimensionless time and frequency variables $\hat{t} = t/t_o$ and $\Delta\hat{f} = \Delta f t_o$. As seen, the

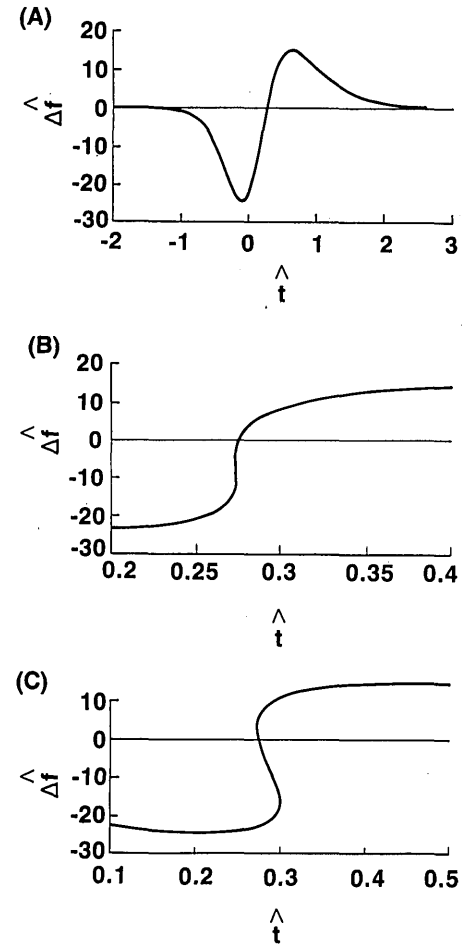

Fig. 7. (A) Calculated instantaneous frequency profile of spectrally broadened pulse considered in Fig. 6(B). (B) Compressed instantaneous frequency profile, with compressor constant $c = 0.034$. (C) Compressed instantaneous frequency, with $c = 0.041$. The variables are $\hat{t} = t/t_o$ and $\Delta\hat{f} = \Delta f t_o$.

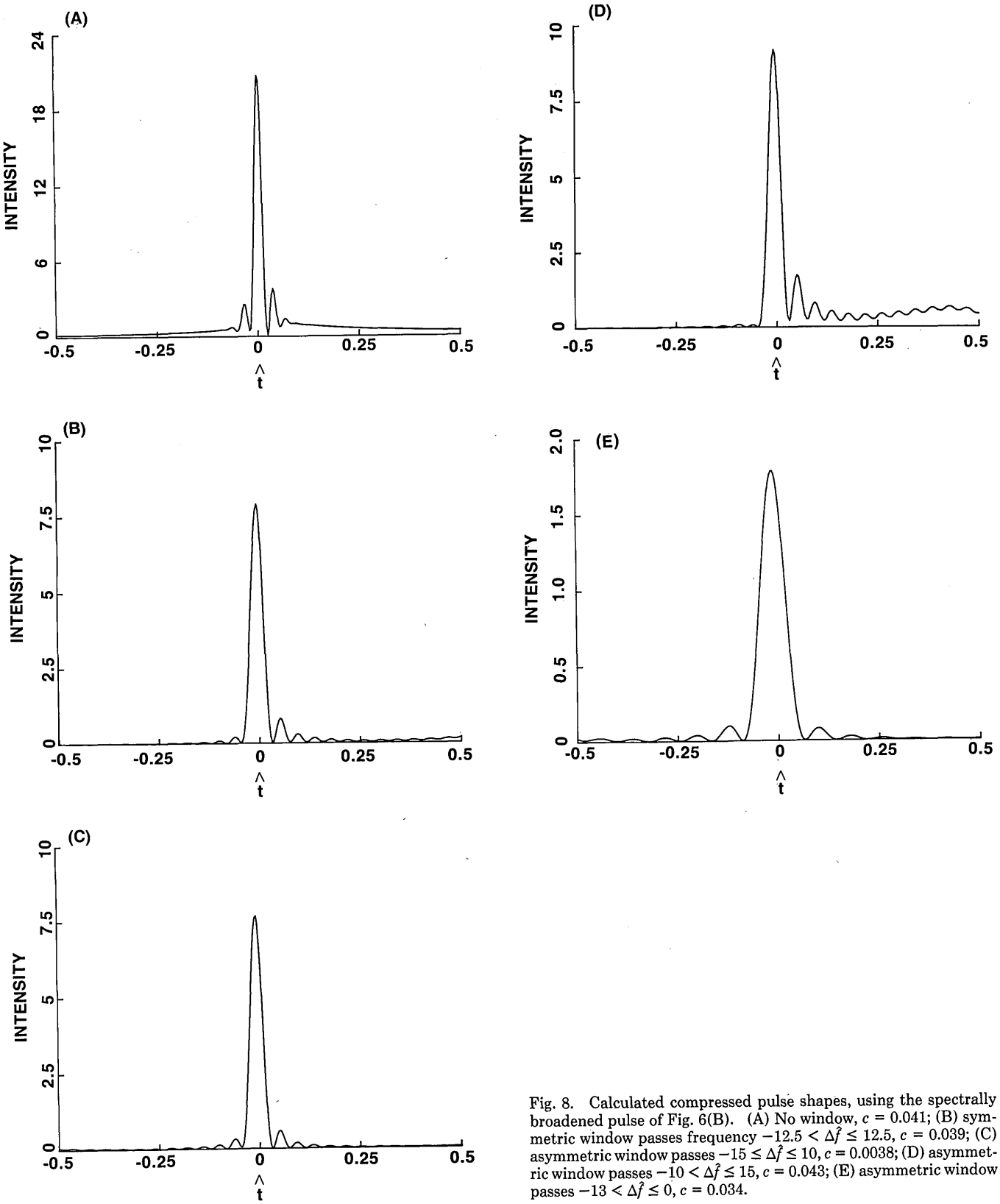

Fig. 8. Calculated compressed pulse shapes, using the spectrally broadened pulse of Fig. 6(B). (A) No window, $c = 0.041$; (B) symmetric window passes frequency $-12.5 < \Delta\hat{f} \leq 12.5$, $c = 0.039$; (C) asymmetric window passes $-15 \leq \Delta\hat{f} \leq 10$, $c = 0.0038$; (D) asymmetric window passes $-10 < \Delta\hat{f} \leq 15$, $c = 0.043$; (E) asymmetric window passes $-13 < \Delta\hat{f} \leq 0$, $c = 0.034$.

region of linear chirp is shifted away from the point $\Delta\hat{f} = 0$ toward the red-shifted portion of the spectrum. This fact is emphasized by replotting the instantaneous frequency profile after taking into account pulse compression by the grating pair. The gratings apply a quadrative factor $e^{ic\Delta\hat{f}^2}$, which imparts to a frequency $\Delta\hat{f}$ a relative group delay equal to $-c\Delta\hat{f}/\pi$. A point $(\hat{t}, \Delta\hat{f})$ in Fig. 7(A) is mapped onto the point $[\hat{t} - (c\Delta\hat{f}/\pi), \Delta\hat{f}]$; c is the compressor factor. The compressed instantaneous frequency is shown in Fig. 7(B) for $c = 0.034$. In the region $-13 < \Delta\hat{f} < 0$, the plot is close to

vertical, indicating perfect compression; but for $\Delta\hat{f} > 0$ the plot rapidly departs from this ideal condition. The highest-intensity compressed pulses are obtained using somewhat larger compression constants, such as $c = 0.041$, as shown in Fig. 7(C). Optimizing the compression involves a compromise between applying perfect phase compensation over a limited bandwidth and applying less than perfect phase compensation but over a larger bandwidth.

Despite the nonlinearity of the frequency chirp, a clean compressed pulse can be generated by using an asymmetric spectral window to select a linearly chirped spectral region. Previously we used a symmetric spectral window[16] to suppress compressed pulse wings in the absence of SRS. Calculated compressed pulses are shown in Fig. 8 without windowing (A), with a symmetric window (B), with a window skewed to the red (C), and with a window skewed to the blue (D). For each window setting, the compressor constant c is adjusted to obtain the most intense compressed pulse. The shortest pulses ($\Delta\hat{t} = 0.02$) are obtained without windowing but are accompanied by extensive wings. The windowed pulses have decreased intensities and increased durations ($\Delta\hat{t} = 0.034$), which are comparable in all three cases. The time–bandwidth product $\Delta f \Delta t$ is approximately 0.80 for (A) and 0.85 for cases (B), (C), and (D). The asymmetric window skewed to the red (C), which coincides most closely with the linear portion of the chirp, eliminates completely the far-out pulse wings. Far-out wings trailing the pulse begin to appear with the symmetric window (B) and become intolerably large with the blue-shifted window (D).

As an aside, we note the large time–bandwidth product in the range 0.8–0.9 obtained in the calculations above. For comparison, $\Delta f \Delta t = 0.315$ for a secant hyperbolic and 0.441 for a Gaussian. To clarify this discrepancy, we performed numerical pulse compression with a tighter window ($-13 < \Delta\hat{f} < 0$) and with $c = 0.034$, corresponding to the "vertical" region in Fig. 7(B). Nearly perfect phase compensation is achieved within this bandwidth. The compressed pulse, shown in Fig. 8(E), has a time–bandwidth product $\Delta f \Delta t = 0.88$. Because the phase compensation is correct, the large $\Delta f \Delta t$ product must arise from the *shape* of the power spectrum. Indeed, the power spectrum is relatively flat in the windowed region and can be approximated as square. The compressed pulse then becomes proportional to $I(t) = \sin^2(\pi \Delta f t)/(\pi \Delta f t)^2$, which has $\Delta f \Delta t = 0.886$, in very good agreement with the numerical calculations. The shape of the compressed pulse in Fig. 8(E), including sidelobes, closely resembles that of the expected sinc function. Experimentally, large time–bandwidth products in the neighborhood of 1.05 have been observed in high-compression-ratio experiments with Nd:YAG lasers[16] and with frequency-doubled Nd:YAG lasers.[18] The large experimental $\Delta f \Delta t$ values would seem to arise mainly because of the flat SPM spectrum and only to a lesser degree because of imperfect compensation of a nonlinear chirp.[27]

We have performed pulse-compression experiments, under conditions of intense SRS, that confirm that high-quality compressed pulses may be obtained with the aid of an asymmetric spectral window. Our experimental findings will be reported in more detail elsewhere.[17] In Fig. 9 we show compressed pulses obtained with an asymmetric spectral window (A) and with no window (B), for ~50% Raman conversion. The contrast is even more dramatic than in the calculations! With the asymmetric window, only frequency components downshifted compared with the center frequency were chosen; a clean pulse with 2-psec duration and minimal wings was obtained. With the window removed (at the same compressor constant), the trace shown in Fig. 9(B) results. This trace is actually the cross-correlation of a short, asymmetrically windowed pulse [such as in Fig. 9(A)] with an unwindowed pulse. In essence, Fig. 9(B) shows a pulse that has been compressed reasonably well on its leading edge but *not* on its trailing edge. Different compressor constants are required to compress one edge of the pulse compared with the other edge. With a single compressor, a clean compressed pulse may be obtained only with a highly asymmetric spectral window.

Pulses, such as that shown in Fig. 9(A), are highly stabilized. Such a pulse displayed on a real-time autocorrelator appears rock solid; fluctuations on its autocorrelation amount to only 1–2%, less than the fluctuations of the mode-locked Nd:YAG laser itself. For comparison, the Nd:YAG laser intensity fluctuations are on the order of 5%. The autocorrelator fluctuations are typically 50% for unwindowed compressed pulses and 10–20% for windowed pulses obtained below the Raman threshold. Stabilized compression is achieved only with strong SRS and with an asymmetric (downshifted) window. Working only slightly above the Raman threshold results in increased fluctuations; removing

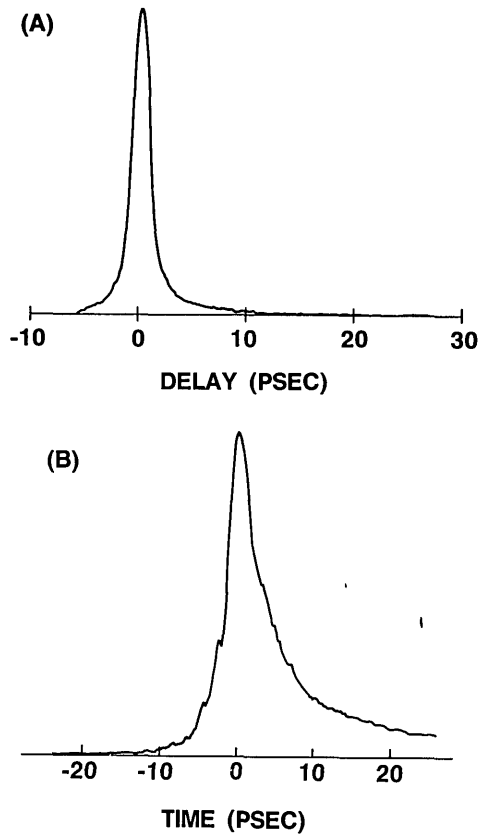

Fig. 9. Experimental compressed pulse shapes obtained under conditions of intense stimulated Raman scattering. (A) Autocorrelation of asymmetrically windowed pulses, with window passing only downshifted spectral components. (B) Measurement of an unwindowed pulse, at the same power level and compressor constant as in (A). This trace is the cross correlation of the unwindowed pulse with the shorter, asymmetrically windowed pulse shown in (A).

the asymmetric window leads to poorly compressed, wingy pulses. Concrete details regarding the performance of our stabilization scheme will be published elsewhere.[17]

Our findings on stabilized pulse compression are closely related to the results of double-slit temporal interference measurements of the optical phase spectrum of compressed pulses, which we reported previously.[28] Those measurements, performed under conditions of strong SRS, indicate that the downshifted frequency components of the pump pulse remain coherent and in phase out to the most extreme frequency shift. The upshifted frequency components, however, maintain uniform phase only over a more restricted interval. At large frequency shifts, the phase of the upshifted spectral components varies rapidly with frequency and loses coherence. These results indicate that the phase spectrum is most uniform and most stable in the spectral region most affected by the stimulated Raman scattering. This is the same spectral region that generates wing-free, stabilized compressed pulses.

Although the exact mechanism responsible for stabilization of the phase spectrum and of pulse compression is not completely established, a number of remarks are possible. First, as shown in Fig. 3, SRS clamps the energy of the incident pulse. Because depletion occurs mainly on the leading edge of the pump pulse, we would suspect that the intensity is stabilized mainly on the leading edge. Second, because the leading edge is sharpened, a large downshifted spectral broadening is obtained within a smaller time window. This would naturally give rise to a more extensive linear chirp region that would be suitable for compression. Finally, GVD may also play a role. In measurements with longer 400-m fibers, with strong SRS, we have observed a regime where GVD strongly influences the red-shifted spectral components but does not significantly affect the blue-shifted frequencies.[17] The increased spectral broadening associated with the steepened pulse rising edge causes GVD to become important for shorter fiber lengths. Even with our short, 145-m fiber, GVD may already assist in linearizing the chirp of the red-shifted spectral components.

5. SUMMARY

We have investigated the influence of strong stimulated Raman scattering on the self-phase modulation of 1.06-μm pulses in single-mode fiber and on grating compression. Walk-off of the generated Stokes pulse through the 1.06-μm pump pulse causes preferential depletion and steepening of the pump rising edge. Subsequent SPM of the asymmetrized 1.06-μm pulses leads to nonsymmetric spectral broadening and a nonlinear chirp. Additionally, stimulated Raman scattering clamps the energy of the pump pulse and stabilizes the phase and amplitude of the downshifted spectral components. By using an asymmetric spectral window to select the stabilized, downshifted spectral region, which corresponds also to the portion of the spectrum most nearly linearly chirped, we have obtained highly stabilized, wing-free compressed pulses. Stabilized compression is achieved only with strong SRS and with an asymmetric window. Without the window, compression results in long, wingy pulses; operating near the Raman threshold leads to increased fluctuations. We are currently investigating in detail the performance of this pulse stabilization scheme and are exploring the role of GVD in the experiments. We anticipate that stabilized compressed pulses will be advantageous to any application in which stability is a concern; specific examples might include generation of seed pulses for high-energy amplifier chains, high-sensitivity optical probing of photodetectors and electronic circuits, and optical communications systems based on frequency-domain coding of individual ultrashort pulses.

ACKNOWLEDGMENT

We are grateful to John Bowers for providing the high-speed photodetector.

REFERENCES AND NOTES

1. R. H. Stolen and C. Lin, "SPM in silica optical fibers," Phys. Rev. A **17,** 1448 (1978).
2. R. H. Stolen, E. P. Ippen, and A. R. Tynes, "Raman oscillation in glass optical waveguide," Appl. Phys. Lett. **20,** 62 (1972).
3. B. Nikolaus and D. Grischkowsky, "90-fs tunable optical pulses obtained by two-stage pulse compression," Appl. Phys. Lett. **43,** 228 (1983).
4. W. J. Tomlinson, R. H. Stolen, and C. V. Shank, "Compression of optical pulses chirped by self-modulation in fibers," J. Opt. Soc. Am. B **1,** 139 (1984).
5. R. H. Stolen, Clinlon Lin, and R. K. Jain, "A time dispersion-tuned fiber Raman oscillator," Appl. Phys. Lett. **30,** 340 (1977).
6. Clinlon Lin and W. G. French, "A near-infrared fiber Raman oscillator tunable from 1.07 to 1.32 μm," Appl. Phys. Lett. **34,** 666 (1979).
7. R. G. Smith, "Optical power handling capacity of low loss optical fibers as determined by stimulated Raman and Brillouin scattering," Appl. Opt. **11,** 2489 (1972).
8. B. Valk, W. Hodel, and H. P. Weber, "Stimulated Raman spectra generated by ps-pulses in a single-mode fiber," Opt. Commun. **54,** (1985).
9. B. Stolz, U. Österberg, A. S. L. Gomes, W. Sibbett, and J. R. Taylor, "Streak camera investigation of Raman pulse generation and propagation in an optical fiber," IEEE J. Lightwave Technol. **LT-4,** 55 (1986).
10. R. H. Stolen and A. M. Johnson, "The effect of pulse walk-off on stimulated Raman scattering in fibers," IEEE J. Quantum Electron. **QE-22,** 2154 (1986).
11. D. Schadt, B. Jaskorzynska, and U. Österberg, "Numerical study on combined stimulated Raman scattering and SPM in optical fibers influenced by walk-off between pump and Stokes pulses," J. Opt. Soc. Am. B **3,** 1257 (1986).
12. A. M. Weiner, J. P. Heritage, and R. H. Stolen, "Effect of stimulated Raman scattering and pulse walk-off on self-phase-modulation in fibers," in *Digest of Lasers and Electro-Optics* (Optical Society of America, Washington, D.C., 1986).
13. B. Zysset and H. P. Weber, "Temporal and spectral investigation of Nd:YAG pulse propagation and its application to pulse compression," in *Digest of Lasers and Electro-Optics* (Optical Society of America, Washington, D.C., 1986).
14. A. S. L. Gomes, W. Sibbett, and J. R. Taylor, "Spectral and temporal study of psec-pulse propagation in a single-mode optical fiber," Appl. Phys. B **39,** 43 (1986).
15. S. L. Palfrey and D. Grischkowsky, "Generation of 16-fsec frequency-tunable pulses by optical pulse compression," Opt. Lett. **10,** 562 (1985).
16. J. P. Heritage, R. N. Thurston, W. J. Tomlinson, A. M. Weiner, and R. H. Stolen, "Spectral windowing of frequency-modulated pulses in a grating compressor," Appl. Phys. Lett. **47,** 87 (1985).
17. J. P. Heritage, A. M. Weiner, and O. E. Martinez, "Stabilized subpicosecond pulse compression due to multiple-order stimulated Raman scattering," J. Opt. Soc. Am. A **4**(13), P56 (1987).
18. A. M. Johnson, R. H. Stolen, and W. M. Simpson, "80× single-stage compression of frequency doubled Nd:yttrium aluminum garnet laser pulses," Appl. Phys. Lett. **44,** 729 (1984).

19. J. P. Heritage, A. M. Weiner, and R. N. Thurston, "Picosecond pulse shaping by spectral phase and amplitude manipulation," Opt. Lett. **10**, 609 (1985).
20. A. M. Weiner, J. P. Heritage, and R. N. Thurston, "Synthesis of phase-coherent, picosecond optical square-pulses," Opt. Lett. **11**, 153 (1986).
21. R. N. Thurston, J. P. Heritage, A. M. Weiner, and W. J. Tomlinson, "Analysis of picosecond pulse shape synthesis by spectral masking in a grating pulse compressor," IEEE J. Quantum Electron. **QE-22**, 682 (1986).
22. J. E. Bowers, C. A. Burrus, and R. J. McCoy, "InGaAs P-I-N photodetectors with modulation response to millimeter wavelengths," Electron. Lett. **21**, 812 (1985).
23. R. L. Fork, O. E. Martinez, and J. P. Gordon, "Negative dispersion using pairs of prisms," Opt. Lett. **9**, 150 (1984).
24. Y. R. Shen and N. Bloembergen, "Theory of stimulated Raman and Brillouin scattering," Phys. Rev. A **137**, 1786 (1985).
25. R. H. Stolen, C. Lee, and R. K. Jain, "Development of the stimulated Raman spectrum in single-mode silica fibers," J. Opt. Soc. Am. B **1**, 652 (1984).
26. R. Cubeddu, R. Polloni, C. A. Sacchi, and O. Svelto, "Self-phase modulation and 'rocking' of molecules in trapped filaments of light with picosecond pulses," Phys. Rev. A **2**, 1955 (1970).
27. In order to obtain the quoted $\Delta f \Delta t$ product of 1.05, we used the formula $\Delta t = \Delta\tau/1.33$, where Δt is the intensity FWHM and $\Delta\tau$ is the autocorrelation FWHM. The conversion factor of 1.33 is appropriate for a square spectrum with uniform phase, as discussed in the text.
28. J. P. Heritage, A. M. Weiner, and R. N. Thurston, "Fourier transform picosecond pulse shaping and spectral phase measurements in a grating pulse-compressor," in *Ultrafast Phenomena V*, G. R. Fleming and A. E. Siegman, eds. (Springer-Verlag, Berlin, 1986), pp. 34–37.

A. M. Weiner

A. M. Weiner was born in Boston, Massachusetts, in 1958. He received the S.B., S.M., and Sc.D. degrees in electrical engineering from the Massachusetts Institute of Technology in 1979, 1981, and 1984, respectively. From 1979 to 1984, he was a Fannie and John Hertz Foundation Graduate Fellow. His doctoral thesis, entitled "Ultrashort Optical Pulse Generation and Dephasing Measurements in Condensed Matter," was awarded the 1984 Hertz Foundation Doctoral Thesis Award. Since 1984 Dr. Weiner has been a member of the technical staff at Bell Communications Research (Bellcore) in Red Bank, New Jersey. At Bellcore he has worked on optical probing of picosecond electronics, nonlinear optics in fibers, and pulse compression and shaping. Most recently his research has focused on high-resolution shaping of femtosecond pulses and applications to time-resolved spectroscopy and to optical communications and switching.

J. P. Heritage

J. P. Heritage received the B.S. degree in electrical engineering from the University of California, Berkeley, in 1967, the M.S. degree in physics from San Diego State University, San Diego, California, in 1971, and the Ph.D. degree in electrical engineering from the University of California, Berkeley, in 1975. From 1975 to 1976, he was with the physics department of the Technical University of Munich, West Germany, as a postdoctoral fellow of the Alexander von Humbouldt Stiftung, where his studies concentrated on picosecond lifetime measurements in organic compounds. In 1976 he joined the staff of Bell Laboratories, Holmdel, New Jersey, where he was a member of the technical staff. Since January 1, 1984, he has been with Bell Communications Research, Inc., where he joined the Physics and Optical Sciences Research Division. His research has led to contributions to the development of high-sensitivity spectroscopy using synchronized, tunable picosecond lasers, vibrational stimulated Raman spectroscopy of surface monolayers, and surface-enhanced nonlinear optics. Subsequently, he has investigated rapid carrier recombination in compound and layered semiconductors and its importance to the problem of temperature sensitivity of threshold in quaternary semiconductor lasers. His recent work has focused on picosecond pulse compression and on a technique for synthesizing arbitrarily shaped picosecond and subpicosecond pulses by using the fiber and grating pulse compressor. His present interests include ultrafast processes in multi-quantum-well structures and compound semiconductors, picosecond and femtosecond spectroscopy with tailored pulse shapes, multigigabit optical communications, fiber nonlinear optics, and infrared picosecond lasers. Dr. Heritage is currently an associate editor of the IEEE Journal of Quantum Electronics. He is a member of the American Physical Society, the Optical Society of America, and the IEEE.